



ELSEVIER

Contents lists available at ScienceDirect

## Redox Biology

journal homepage: [www.elsevier.com/locate/redox](http://www.elsevier.com/locate/redox)

## Method

## An ex-vivo model for evaluating bioenergetics in aortic rings

Kyle P. Feeley<sup>a</sup>, David G. Westbrook<sup>a,b</sup>, Alexander W. Bray<sup>a,b</sup>, Scott W. Ballinger<sup>a,b,\*</sup><sup>a</sup> Department of Pathology, Division of Molecular and Cellular Pathology, University of Alabama at Birmingham, Birmingham, AL 35294, USA<sup>b</sup> Center for Free Radical Biology, University of Alabama at Birmingham, Birmingham, AL 35294, USA

## ARTICLE INFO

## Article history:

Received 12 August 2014

Received in revised form

22 August 2014

Accepted 26 August 2014

Available online 3 September 2014

## Keywords:

Mitochondrion

Aorta

Cardiovascular disease

Bioenergetics

Atherosclerosis

## ABSTRACT

Cardiovascular disease (CVD) is the leading cause of death worldwide and it exhibits a greatly increasing incidence proportional to aging. Atherosclerosis is a chronic condition of arterial hardening resulting in restriction of oxygen delivery and blood flow to the heart. Relationships between mitochondrial DNA damage, oxidant production, and early atherogenesis have been recently established and it is likely that aspects of atherosclerotic risk are metabolic in nature. Here we present a novel method through which mitochondrial bioenergetics can be assessed from whole aorta tissue. This method does not require mitochondrial isolation or cell culture and it allows for multiple technical replicates and expedient measurement. This procedure facilitates quantitative bioenergetic analysis and can provide great utility in better understanding the link between mitochondria, metabolism, and atherogenesis.

© 2014 Published by Elsevier B.V. This is an open access article under the CC BY-NC-ND license (<http://creativecommons.org/licenses/by-nc-nd/3.0/>).

## Introduction

Cardiovascular disease (CVD) is the leading cause of death worldwide, and nearly 600,000 deaths were caused by CVD in the United States alone in 2010 [1–3]. Though mortality due to CVD has declined in recent years in high-income countries, incidence has held steady or even increased in many middle and low income countries [4]. CVD mortality exhibits an exponential increase proportional to age and is seen more often in men than in women [4]. Primary prevention strategies, improved treatment options, and policy changes related to addressing risk factors (e.g. reducing tobacco smoke use and exposure) have all contributed to the encouraging trend of diminished CVD related mortality in higher income countries [5]. Part of the problem in adequately managing CVD is that acute myocardial events are often the result of years of asymptomatic disease progression [6]. In view of this, an improved understanding of the processes that contribute to CVD may significantly contribute to additional treatment options or more precise preventative care.

Atherosclerosis is a chronic condition where the innermost layer of the artery becomes hardened and narrowed due to a buildup of plaque [7]. Damaged arterial endothelium accumulates LDL cholesterol and blood-borne monocytes which leads to further inflammation and biochemical modifications [8,9]. The atherosclerotic plaque then begins to clog the artery, making blood flow

and oxygen delivery difficult. If the artery becomes fully occluded, irreversible myocardial cell damage or cell death will occur [7]. Though coronary plaque growth may remain stable for many years, it is also possible for plaques to suddenly rupture, leading to immediate downstream intraluminal thrombi and accelerated blood-flow obstruction resulting in myocardial infarction [10,11]. High blood pressure, high cholesterol, diabetes, obesity, smoking, and a family history of heart disease are all risk factors for atherosclerosis in addition to aging [3,12,13].

Reactive oxygen species (ROS) are chemically reactive molecules formed as a byproduct of oxidative metabolism which serve important roles in homeostasis and cell signaling as well as increasingly appreciated functions in various pathologies [14–16]. Epidemiological studies support an association between increased ROS levels and common CVD risk factors [17,18]. More recently, mitochondrial function and reactive species production have also been implicated in atherogenesis [19,20]. Exposure of vascular cells to ROS results in mitochondrial DNA (mtDNA) damage and dysfunction which negatively affects the metabolic phenotype, subsequently resulting in endothelial cell dysfunction and smooth muscle cell disturbances [21]. The idea that mtDNA damage accumulation is an initiating event in atherogenesis is additionally consistent and complementary with popular inflammatory response theories [7,22,23]. Previously, assays directed toward determining the extent of mtDNA damage were used to investigate early atherogenesis [20]. Using that approach is a helpful way to characterize damaged mtDNA, but a more complete and quantitative picture may yet be obtained.

\* Correspondence to: BMR2 530, 1720 2nd Avenue South, Birmingham, AL 35294-2180, USA.

E-mail address: [sballing@uab.edu](mailto:sballing@uab.edu) (S.W. Ballinger).

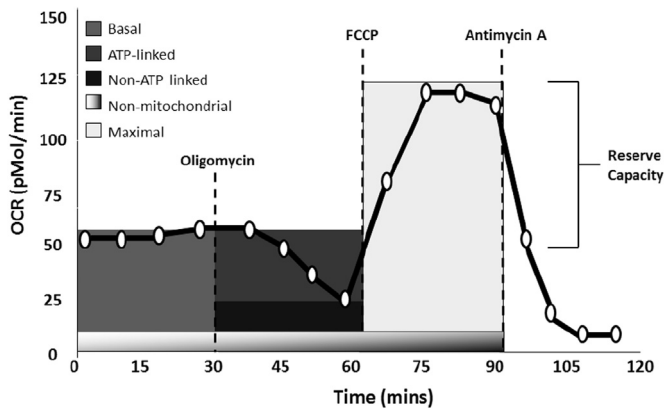


**Fig. 1.** Example experimental trace result from the XF24 depicting oxygen consumption rate (OCR) of an ex-vivo aortic ring in response to a sequence of metabolic effectors. Following measurement of baseline oxygen consumption, oligomycin is added to inhibit ATP synthase which initiates a decline in oxygen consumption, thus delineating between oxygen consumption that is linked (ATP-linked) or not linked to ATP production (non-ATP). FCCP is a mitochondrial uncoupling agent which facilitates maximal oxygen consumption, while antimycin A is a potent inhibitor of electron transport complexes III. The difference between the maximal OCR following FCCP and the baseline OCR is the reserve capacity.

The Seahorse XF bioanalyzer is a platform that allows oxygen consumption and extracellular acidification to be measured from tissue in response to specific electron transport chain effectors in real time [24]. By doing this, bioenergetic profiles can be generated that further enable investigation into the role of metabolic differences on cardiovascular disease susceptibility and progression. ATP-linked respiration, maximal respiration, reserve capacity, and non-mitochondrial oxygen consumption are all parameters that can be measured over a single experiment in addition to baseline respiration (Fig. 1) [24,25]. Herein, we present an assay enabling generation of bioenergetic profiles using an ex vivo method from isolated aortic sections taken from apolipoprotein E null (*apoE*<sup>-/-</sup>) mice fed either a chow diet or a western high fat diet. ApoE is a lipoprotein receptor ligand responsible for LDL uptake that, when missing, as in the *apoE* mouse, leads to elevated serum LDL cholesterol levels and atherosclerotic lesion development [26,27].

## Methods

All procedures and manipulations of animals were approved by the Institutional Animal Care and Use Committee (IACUC) of the University of Alabama at Birmingham in accordance with the United States Public Health Service Policy on the humane Care and Use of Animals, and the NIH Guide for the Care and Use of Laboratory Animals.

## Seahorse XF24 preparation

1.0 mL of Seahorse Bioscience XF24 Calibrant pH 7.4 (#100840-000, Seahorse Bioscience, North Billerica, MA) was added to each well of a Seahorse Bioscience 24-well plate (#100777-004) that is kept overnight at room temperature.

## Mice

C57BL/6J *apoE*<sup>-/-</sup> male mice (002052) were purchased from Jackson Laboratories in Bar Harbor, Maine. All mice were fed chow diets (4% fat: Harlan Teklad diet 7001) until 6 weeks old when half remained on chow and the other half were fed a western high fat diet (21% fat: Harlan Teklad diet 88137) for 10 weeks until sacrifice at 16 weeks. Four mice, two from each diet group, were sacrificed on the same day for aorta removal and Seahorse plate preparation.

## Aortic isolation

Mice were sacrificed at 16 weeks of age via prolonged exposure to a dose of isoflurane followed by cervical dislocation. The aorta was removed and placed into a 100 × 20 mm<sup>2</sup> cell culture dish containing 1 mL of unbuffered DMEM. Under a dissecting microscope, exterior fat and extraneous branching arteries were carefully removed (Fig. 2). Next, the aorta was cleaned, opened longitudinally, and cut into equal pieces 3 mm in length (in this manner, the typical aorta provides 4 pieces).

## Seahorse XF-24 protocol

Aortic sections were placed into individual wells on an XF24 cell culture plate pre-warmed with unbuffered DMEM (250 μL, 37 °C), leaving appropriate temperature correction wells blank (A1, B4, C3, D6). Tissue was incubated in the XF24 cell culture plate in a 37 °C incubator without CO<sub>2</sub> until ready for use to allow aortic sections to equilibrate to the new media. Injection compound dilutions were made in appropriate running media (unbuffered DMEM) for the bioenergetic profile analysis experiment. Initially, titration experiments were run to determine each effector's appropriate working concentration. For these studies, optimal concentrations were found to be: 10 μg/mL Oligomycin, 1 μM FCCP (Trifluorocarbonyl cyanide Phenylhydrazine), and 10 μM Antimycin A.

Oligomycin, FCCP, Antimycin A, and media were loaded into injection ports A, B, C, and D, respectively, in 75 μL volumes for each experimental well. All wells, including temperature correction wells, had control media or compounds loaded into all ports to ensure uniform injection. Once prepared, the plate containing the effectors was placed atop the plate containing the aorta samples and placed into the XF24 Bioanalyzer. Each oxygen consumption rate (OCR) measurement consisted of 3 min of

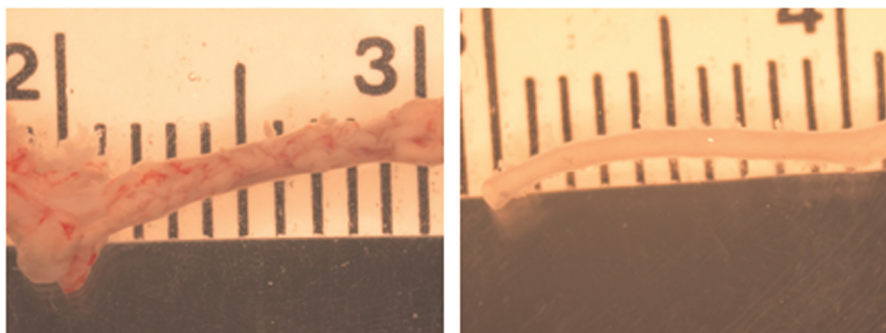


**Fig. 2.** Images depicting an isolated aorta (A) before and (B) after removing extraneous fat.

mixing, 2 min wait time, and 3 min of continuous O<sub>2</sub> level measurement. There were 3 measurement rounds per injection.

### Data analysis and interpretation

The Seahorse XF-24 outputs experimental data as a connected scatter plot with either Oxygen Consumption Rate (OCR) or Extracellular Acidification Rate (ECAR) on the y-axis and time on the x-axis. Once converted into a table format, the data from each sample was divided into four blocks corresponding to each effector injection: basal, oligomycin, FCCP, and antimycin-A. The relevant measures for each block was as follows: basal average, oligomycin minimum, FCCP maximum, and antimycin-A minimum. These values were used to determine the OCRs at baseline, linked to ATP, not linked to ATP (non-ATP), at maximal levels, and the reserve capacity. ATP-linked oxygen consumption was determined by finding the difference between the baseline OCR and the post-oligomycin minimum OCR; the value of the post-oligomycin minimum represents the OCR not linked to ATP generation (non-ATP). The maximum OCR is determined from the maximum value of post-FCCP OCR. Lastly, reserve capacity was the difference between the baseline and maximum OCRs.

Variation between individual Seahorse wells containing pieces of the same aorta is present in these experiments. For these studies the coefficient of variation (CV) had a range from 0.06 to 0.7, with an average of 0.2. This compares quite favorably to a recent *ex vivo* method for using adipose tissues published by our group [28].

## Results

This report details the development of an assay that enables real-time quantification of oxygen utilization and extracellular acidification from *ex-vivo* aortic slices. In preliminary analyzes comparing bioenergetic profiles between apoE<sup>-/-</sup> mice that were either fed a standard chow diet or a western high fat diet, the mice on high fat diet had a higher basal OCR than their chow-fed counterparts (Fig. 3). The component parts of these different baseline measures are also different. The chow-fed animals have a baseline OCR that is 32% ATP-linked and 68% non-ATP-linked whereas the HFD-fed animals have a baseline OCR that is 41% ATP-linked and 59% non-ATP-linked (Fig. 4). Further dissection of changes in bioenergetics capacities suggested that changes in

“reserve capacity” occurred between chow and high fat diet groups (Fig. 4). Reserve capacity is a measure of the difference between the maximum possible OCR (following FCCP addition) and the baseline OCR. This parameter is proposed to be a measure of the ability of cells or tissue to respond to stresses by increasing their metabolic output. When incorporating this parameter into the observed bioenergetics it revealed that under maximal oxygen consumption rates (FCCP induced), reserve capacity accounted for 60% and 56% of the maximum OCR for chow and high fat diet animals, respectively, and oxygen utilization for ATP generation to be 13% and 18% in chow and high fat groups, respectively (Fig. 4).

## Discussion and conclusions

Given that cardiovascular disease is the leading cause of death worldwide in both men and in women, the need to better investigate and understand mechanisms of atherosclerosis is a priority in the medical research world. The purpose of this study was to develop a robust, efficient, and reproducible method for evaluating tissue bioenergetics from *ex-vivo* aorta. Such an assay could then be used to directly observe the metabolic phenotype of aortic sections, thus allowing for a wide range of experimental designs directed toward deepening our understanding of the role of metabolism in cardiovascular disease risk and progression.

An important point when considering normalizing these experimental data is that equally sized aortic slices may not contain the same amount of mitochondria. This is especially true in the case of comparing healthy to diseased aortas, or when comparing the bioenergetics of aortas taken from mice on different genetic backgrounds. While differences in mitochondrial numbers are normalized when determining relative percent OCR dedicated for ATP, non-ATP, and reserve capacity, when reporting actual OCR, it can be necessary to normalize all bioenergetic data against mtDNA copy number. This can be done via quantification of mtDNA copy numbers, described previously [29].

The observed changes in bioenergetics in aortic ring tissues collected from chow and high fat diet fed mice represent a categorical “mean” of that tissue. While tissue orientation is endothelial “side-up” for this method, OCR could be affected by additional associated cells linked to disease pathology such as macrophage and proliferating smooth muscle cells. In this respect, qualitatively determining thresholds for healthy and unhealthy aorta would be disease-model specific. For concerns regarding attributing differences in bioenergetics to specific cell types, OCR data could be normalized against cell specific markers. Alternatively, primary cells could be isolated; however this approach precludes *ex vivo* measures, and also has drawbacks of cell fitness and selection during culture expansion. Using this *ex vivo* approach, we show that high fat diet feeding in apoE<sup>-/-</sup> mice decreases reserve capacity and increases OCR for ATP production in aortic rings, compared to chow fed apoE<sup>-/-</sup>. To further delineate interpretation, mitochondrial DNA damage analysis could be performed post hoc on the same tissue samples to assess both mtDNA damage and total mitochondrial number (as mentioned previously) in the tissue, as well as total DNA content to estimate cellularity, and as previously suggested, cell specific markers to determine relative ratios of cell types.

This method is distinct from previously published strategies designed to investigate potential links between oxidative damage, metabolic phenotype, and atherosclerotic risk in that there is no need for mitochondrial isolation or cell culture using the *ex vivo* method, and this technique can be performed quickly and reproducibly. Furthermore, directly measuring bioenergetics from primary aortic tissues precludes complications that arise from unnecessary additional sample manipulation. Having several

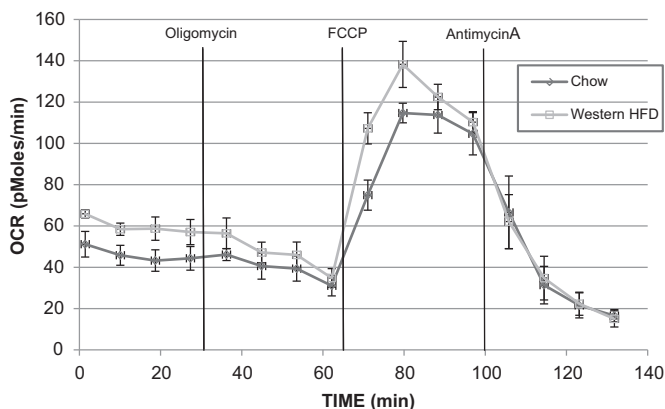


**Fig. 3.** Oxygen consumption rates in *ex-vivo* aortic sections taken from 16-week old apoE<sup>-/-</sup> mice fed either chow or a high fat diet. Traces are from a single experiment using 2 mice per group with 4 replicates per mouse (i.e. 4 aortic sections per mouse). OCR is measured under basal conditions as well as following addition of oligomycin, FCCP, and antimycin A. Each data point is the average of four independent measurements. Error bars indicate  $\pm$  S.E.M.



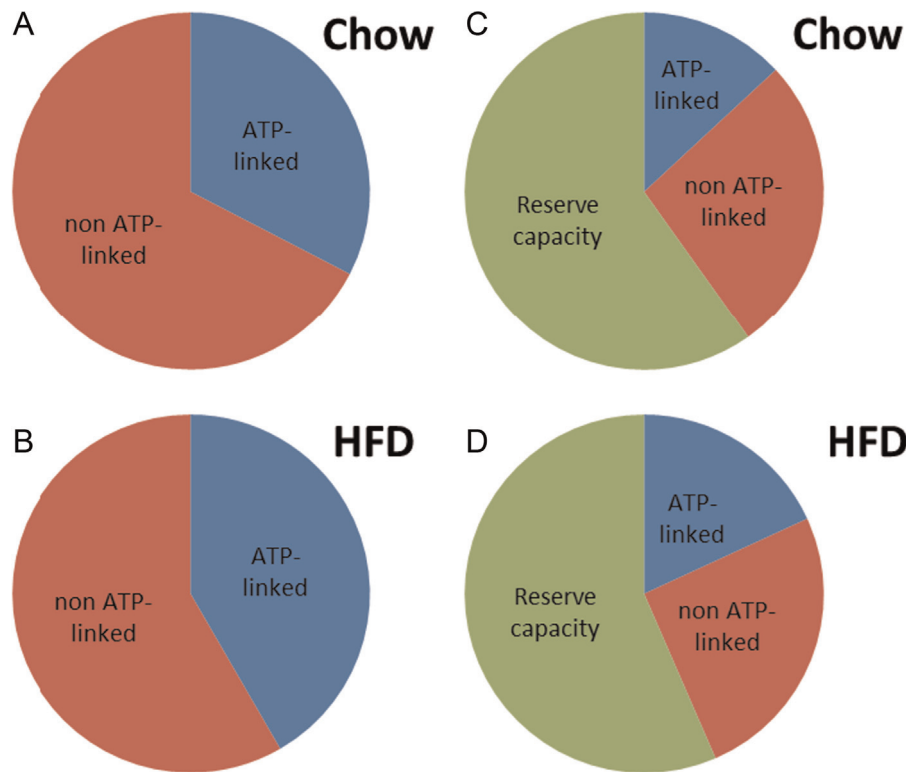


**Fig. 4.** Pie charts indicating oxygen utilization profiles of aortic sections for chow and high-fat fed apoE<sup>-/-</sup> mice from 4 individual experiments. The left side displays the percentage of basal oxygen consumption that is linked to ATP production and non-ATP production for chow (A) and high fat fed (B) animals. The right side displays the percentage of maximal oxygen consumption that is linked to reserve capacity, ATP production, or non-ATP production for chow (C) and high fat fed (D) animals.

technical replicates per mouse as well as several mice per group analyzed simultaneously provides the benefit of addressing any potential experimental variation. Beyond its utility in examining mouse aorta, this ex-vivo bioenergetic approach could be extended for use in vascular biopsies taken from surgical specimens, or even in a prophylactic setting to improve diagnostics. As suggested in these studies, we would anticipate decreased reserve capacity with pathology progression, often associated with increased oxygen consumption under basal conditions.

### Acknowledgements

This study was funded by NIH Grant HL103859 (S.W.B.) and an NHLBI pre-doctoral training Grant T32HL007918 in Cardiovascular Pathophysiology (A.W.B.).

### References

- [1] V. Fuster, B.B. Kelly, *Promoting Cardiovascular Health in the Developing World: A Critical Challenge to Achieve Global Health*, National Academies Press, Washington, DC, 2010.
- [2] Heron, M., Deaths: leading causes for 2010. National Vital Statistics Reports, vol. 62 (6), 2013.
- [3] A.S. Go, et al., Heart disease and stroke statistics – 2014 update: a report from the American Heart Association, *Circulation* 129 (3) (2014) e28–e292. <http://dx.doi.org/10.1161/01.cir.0000441139.02102.80> 24352519.
- [4] J.A. Finegold, et al., Mortality from ischaemic heart disease by country, region, and age: statistics from World Health Organisation and United Nations, *International Journal of Cardiology* 168 (2) (2013) 934–945. <http://dx.doi.org/10.1016/j.ijcard.2012.10.046> 23218570.
- [5] A.S. Daar, et al., Grand challenges in chronic non-communicable diseases, *Nature* 450 (7169) (2007) 494–496. <http://dx.doi.org/10.1038/450494a> 18033288.
- [6] R. Ross, The pathogenesis of atherosclerosis: a perspective for the 1990s, *Nature* 362 (6423) (1993) 801–809. <http://dx.doi.org/10.1038/362801a0> 8479518.
- [7] G.K. Hansson, Inflammation, atherosclerosis, and coronary artery disease, *New England Journal of Medicine* 352 (16) (2005) 1685–1695. <http://dx.doi.org/10.1056/NEJMr043430> 15843671.
- [8] C. Schulz, S. Massberg, Atherosclerosis – multiple pathways to lesional macrophages, *Science Translational Medicine* 6 (239) (2014) 1–5.
- [9] J.L. Witztum, A.H. Lichtman, The influence of innate and adaptive immune responses on atherosclerosis, *Annual Review of Pathology* 9 (2014) 73–102. <http://dx.doi.org/10.1146/annurev-pathol-020712-163936> 23937439.
- [10] L.H. Arroyo, R.T. Lee, Mechanisms of plaque rupture: mechanical and biologic interactions, *Cardiovascular Research* 41 (2) (1999) 369–375. [http://dx.doi.org/10.1016/S0008-6363\(98\)00308-3](http://dx.doi.org/10.1016/S0008-6363(98)00308-3) 10341836.
- [11] K. Thygesen, et al., Third universal definition of myocardial infarction, *Journal of the American College of Cardiology* 60 (16) (2012) 1581–1598. <http://dx.doi.org/10.1016/j.jacc.2012.08.001>.
- [12] D. Anthony, et al., Cardiac risk factors: new cholesterol and blood pressure management guidelines, *FP Essentials* 421 (2014) 28–43 24936717.
- [13] N.J. Wald, M.R. Law, A strategy to reduce cardiovascular disease by more than 80%, *British Medical Journal* 326 (7404) (2003) 1419. <http://dx.doi.org/10.1136/bmj.326.7404.1419> 12829553.
- [14] P.S. Brookes, et al., Mitochondria: regulators of signal transduction by reactive oxygen and nitrogen species, *Free Radical Biology & Medicine* 33 (6) (2002) 755–764. [http://dx.doi.org/10.1016/S0891-5849\(02\)00901-2](http://dx.doi.org/10.1016/S0891-5849(02)00901-2) 12208364.
- [15] K. Ishikawa, et al., ROS-generating mitochondrial DNA mutations can regulate tumor cell metastasis, *Science* 320 (5876) (2008) 661–664. <http://dx.doi.org/10.1126/science.1156906> 18388260.
- [16] G.C. Chuang, et al., Pulmonary ozone exposure induces vascular dysfunction, mitochondrial damage, and atherogenesis, *American Journal of Physiology. Lung Cellular and Molecular Physiology* 297 (2) (2009) L209–L216. <http://dx.doi.org/10.1152/ajplung.00102.2009> 19395667.
- [17] H. van Jaarsveld, et al., Exposure of rats to low concentration of cigarette smoke increases myocardial sensitivity to ischaemia/reperfusion, *Basic Research in Cardiology* 87 (1992) 393–399. <http://dx.doi.org/10.1007/BF00796524> 1417708.
- [18] R.W. Alexander, Atherosclerosis as disease of redox-sensitive genes, *Transactions of the American Clinical and Climatological Association* 109 (1998) 129–145 9601133.
- [19] S.W. Ballinger, et al., Hydrogen peroxide- and peroxynitrite-induced mitochondrial DNA damage and dysfunction in vascular endothelial and smooth muscle cells, *Circulation Research* 86 (9) (2000) 960–966. <http://dx.doi.org/10.1161/01.RES.86.9.960> 10807868.
- [20] S.W. Ballinger, et al., Mitochondrial integrity and function in atherogenesis, *Circulation* 106 (5) (2002) 544–549. <http://dx.doi.org/10.1161/01.CIR.0000023921.93743.89> 12147534.

- [21] C.M. Harrison, et al., Mitochondrial oxidative stress significantly influences atherogenic risk and cytokine-induced oxidant production, *Environmental Health Perspectives* 119 (5) (2011) 676–681. <http://dx.doi.org/10.1289/ehp.1002857> 21169125.
- [22] T. Oka, et al., Mitochondrial DNA that escapes from autophagy causes inflammation and heart failure, *Nature* 485 (7397) (2012) 251–255. <http://dx.doi.org/10.1038/nature10992> 22535248.
- [23] E. Yu, et al., Mitochondria in vascular disease, *Cardiovascular Research* 95 (2) (2012) 173–182. <http://dx.doi.org/10.1093/cvr/cvs111> 22392270.
- [24] B.P. Dranka, et al., Assessing bioenergetic function in response to oxidative stress by metabolic profiling, *Free Radical Biology & Medicine* 51 (9) (2011) 1621–1635. <http://dx.doi.org/10.1016/j.freeradbiomed.2011.08.005> 21872656.
- [25] B.P. Dranka, et al., Mitochondrial reserve capacity in endothelial cells: The impact of nitric oxide and reactive oxygen species, *Free Radical Biology & Medicine* 48 (7) (2010) 905–914. <http://dx.doi.org/10.1016/j.freeradbiomed.2010.01.015> 20093177.
- [26] A.S. Plump, et al., Severe hypercholesterolemia and atherosclerosis in apolipoprotein E-deficient mice created by homologous recombination in ES cells, *Cell* 71 (1992) 343–353. [http://dx.doi.org/10.1016/0092-8674\(92\)90362-G](http://dx.doi.org/10.1016/0092-8674(92)90362-G) 1423598.
- [27] Y. Nakashima, et al., ApoE-deficient mice develop lesions of all phases of atherosclerosis throughout the arterial tree, *Arteriosclerosis and Thrombosis: A Journal of Vascular Biology* 14 (1994) 133–140.
- [28] K.J. Dunham-Snary, et al., A method for assessing mitochondrial bioenergetics in whole white adipose tissues, *Redox Biology* 2 (2014) 656–660. <http://dx.doi.org/10.1016/j.redox.2014.04.005> 24936439.
- [29] D.G. Westbrook, et al., Perinatal tobacco smoke exposure increases vascular oxidative stress and mitochondrial damage in non-human primates, *Cardiovascular Toxicology* 10 (3) (2010) 216–226. <http://dx.doi.org/10.1007/s12012-010-9085-8> 20668962.